*Journal of Physiology* (1988), **407**, *pp.* 293–310
*With 8 text-figures*
*Printed in Great Britain*



# ELECTROPHYSIOLOGICAL PROPERTIES OF ROSTRAL MEDULLARY RESPIRATORY NEURONES IN THE CAT: AN INTRACELLULAR STUDY

BY A. L. BIANCHI*, L. GRÉLOT, S. ISCOE† AND J. E. REMMERS

*From the Département de Physiologie et Neurophysiologie, Faculté des Sciences Saint-Jérôme, Marseille, France and the Respiratory Research Group, Faculty of Medicine, University of Calgary, Calgary, Canada*

(*Received 16 March 1988*)

SUMMARY

1. We recorded the membrane potentials of sixty-three respiratory neurones in the rostral, ventral medulla of decerebrate vagotomized cats. Stable recordings were obtained in thirty-eight expiratory and twenty-five inspiratory neurones. Axonal projections were identified by antidromic invasion after electrical stimulation of the region of the dorsal respiratory group (DRG), spinal cord, and the cervical vagus, superior laryngeal and pharyngeal nerves.

2. Two types of expiratory neurones were encountered: those in which the membrane potential progressively depolarized (augmenting neurones, $n = 22$) and those in which the membrane potential repolarized (decrementing or post-inspiratory neurones, $n = 16$) during the interval between phrenic bursts. Both types were hyperpolarized during inspiration by chloride-dependent, inhibitory postsynaptic potentials (IPSPs) which decreased membrane resistance. In augmenting neurones two waves of IPSPs appeared, one early and one late in inspiration.

3. Five out of seventeen augmenting expiratory neurones tested were antidromically activated by contralateral stimulation of the spinal cord ($n = 3$) or the DRG ($n = 2$). Spinal axons were not detected in any of the sixteen decrementing expiratory neurones tested. Of thirteen expiratory neurones tested with pharyngeal nerve stimulation, one (an augmenting type) was antidromically activated. Superior laryngeal or vagal axons could not be demonstrated for any expiratory neurones.

4. Two types of inspiratory neurones were also encountered: those displaying progressive depolarization throughout inspiration ($n = 5$) and those which gradually repolarized after maximal depolarization at the onset of inspiration ($n = 10$). None of the former had identifiable spinal or medullary axons, but superior laryngeal axons were demonstrated in three and pharyngeal axons were found in three. None of the latter was antidromically activated from any of the sites stimulated.

5. Stimulation of the superior laryngeal or pharyngeal nerves evoked excitatory postsynaptic potentials (EPSPs) in all neurones except in post-inspiratory neurones.

* To whom all correspondence and reprint requests should be sent at Laboratoire de Neurobiologie de la Respiration, Case 351, Faculté des Sciences et Techniques Saint-Jérôme, Avenue Escadrille Normandie-Niemen, 13397 Marseille, Cedex 13, France.

† Present address: Department of Physiology, Queen's University, Kingston, Ontario K7L 3N6, Canada.

In these, stimulation of the superior laryngeal or pharyngeal nerves evoked IPSPs in five of twelve neurones tested.

6. We conclude that a spectrum of respiratory neurones lie within or ventral to the retrofacial nucleus. These neurones may control upper-airway muscles or may play a role in chemoreception.

## INTRODUCTION

Respiratory rhythm in mammals probably results from synaptic interactions between respiratory neurones located in the lower brain stem (for references see Long & Duffin, 1986). Until recently, most of these neurones were presumed to lie solely within the dorsal and ventral groups of respiratory neurones. The dorsal group includes inspiratory bulbospinal neurones lying in the ventrolateral nucleus of the solitarius tract (von Baumgarten, von Baumgarten & Schaeffer, 1957; Bianchi, 1971; von Euler, Hayward, Marttila & Wyman, 1973). The ventral group consists of inspiratory and expiratory neurones lying in a region associated with the nucleus paraambiguus and retroambigalis in the vicinity of the nucleus ambiguus and having bulbospinal or propriobulbar axons (Batsel, 1964; Merrill, 1970; Bianchi, 1971). Recently, a third group of respiratory neurones, at the rostral extension of the ventral respiratory group, has been identified by neuroanatomical (Kalia, Feldman & Cohen, 1979 ; Bystrzycka, 1980) and electrophysiological (Lipski & Merrill, 1980; Bianchi & Barillot, 1982; Fedorko & Merrill, 1984) studies. This group includes the so-called 'Bötzinger complex' which consists primarily of expiratory neurones (Lipski & Merrill, 1980) and the retrofacial group, including respiratory neurones of both the 'Bötzinger complex' and the retrofacial nucleus (Bianchi & Barillot, 1982; Bianchi, 1985).

Extracellular recordings of respiratory neurones of this region have demonstrated the existence of expiratory neurones with augmenting discharge patterns which appear to be the source of postsynaptic inhibition of inspiratory pre-motoneurones and motoneurones (Merrill, Lipski, Kubin & Fedorko, 1983; Fedorko & Merrill, 1984). In addition, other types of respiratory neurones exist in the region of the retrofacial nucleus. These include early burst inspiratory and early expiratory (post-inspiratory) neurones with decrementing discharge patterns, inspiratory neurones with augmenting discharge patterns, and phase-spanning neurones (Lipski & Merrill, 1980; Bianchi & Barillot, 1982; Bianchi, 1985; Remmers, Takeda, Schultz & Haji, 1985*b*). Some of these may be motoneurones of upper-airway muscles, the cell bodies of which lie in the rostral part of the nucleus ambiguus or in the retrofacial nucleus itself. In the present study, we wished to examine in these rostral bulbar respiratory neurones their changes in membrane potential and patterns of spontaneous and evoked postsynaptic potentials, identify their axonal projections, and relate these characteristics to their morphology and location. Some of these results have been reported in abstract form (Bianchi, Grélot & Remmers, 1987).

## METHODS

Experiments were performed on twenty-six cats of either sex weighing 2·2–4·5 kg. The animals were initially anaesthetized with an intramuscular injection of 1·5 ml/kg of a mixture of Alfaxalone and Alfadolone acetate (9 and 3 mg/ml respectively; Saffan, Glaxovet) to permit cannulation of the trachea and femoral veins and arteries, and bilateral ligation of the external carotid arteries.

Anaesthesia was then maintained with halothane. Phrenic nerve rootlets were dissected in the neck and both vagus nerves cut at the mid-cervical level.

The animals were then placed in a stereotaxic frame and decerebrated mid-collicularly (Kirsten & St John, 1978). After occipital craniotomy, the cerebellum was gently retracted or its caudal portion removed by aspiration. A dorsal laminectomy was performed from C3 to C7. The animals were then paralysed with gallamine triethiodide (2 mg/kg I.V., supplemented as required) and artificially ventilated with $O_2$-enriched air to maintain the fractional $CO_2$ concentration of end-tidal gas between 0·04 and 0·05. Respiratory movements of the brain stem were prevented by a bilateral pneumothorax, and a positive end-expiratory pressure of 2–5 $cmH_2O$ was applied to prevent collapse of the lungs. Halothane was then discontinued and a minimum of 1 h was allowed to elapse before respiratory activities were recorded. Mean femoral arterial pressure was at least 80 mmHg in all experiments. The rectal temperature was maintained between 36 and 38 °C by a servo-controlled heating pad. Infusion of isotonic sodium bicarbonate corrected any metabolic acidosis which was usually evidenced by a gradual fall in blood pressure.

*Recording and stimulation*

The C5 phrenic nerve rootlets were cut distally on both sides, desheathed, and placed on bipolar platinum electrodes immersed in mineral oil. Action potentials from these nerves were amplified, rectified and 'integrated' with a resistance–capacitance circuit (time constant 100 ms) and used to monitor the neural respiratory cycle.

Intracellular potentials with patterns of activity linked to the bursts of phrenic nerve activity were recorded through glass micropipettes filled with 3 M-potassium chloride solution or a 10% solution of horseradish peroxidase (HRP, Sigma VI) in 0·5 M-potassium chloride buffered at pH 8·0–8·6. Microelectrodes tips were broken to a maximal outer diameter of 1·0 $\mu$m before filling. Resistances, measured at 100 Hz, ranged from 8 to 15 MΩ for micropipettes filled with potassium chloride and from 15 to 30 MΩ for those filled with horseradish peroxidase solution. The micropipette was inserted vertically through a pressure foot on the dorsal surface. Respiratory neurones were impaled 3·5–6·0 mm below the dorsal surface of the brain stem. They were located 2·9–3·75 mm lateral to the mid-line and 3·4–5·7 mm rostral to the obex.

Intracellular potentials were amplified through a high-impedance circuit incorporating capacity compensation, DC offset, and a bridge circuit for current injection across the recording microelectrode (Dagan 8100 or Transidyne 1600). DC recordings of membrane potential were displayed continuously at low ( × 10) and variable high amplification on a chart recorder together with integrated phrenic nerve activity. All data were stored on magnetic tape (bandwidth 0–5 kHz). Records presented were obtained by playing back the signals to a pen-writer (Gould 2000 W) or an electrostatic (Gould ES 1000) recorder. They were also available as $X$–$Y$ plots of the output from a digital oscilloscope (Nicolet 3091) or computer (IBM AT) using appropriate software (RC Electronics, ComputerScope).

In order to identify the axonal projections of the impaled respiratory neurones, electrical stimuli (duration, 0·1 ms) were systematically delivered via bipolar electrodes to the ipsilateral cervical vagus and superior laryngeal nerves (0·5–4·0 V), and bilaterally to the cervical spinal cord (5–25 V) through an array of six concentric bipolar electrodes (Rhodes, SNE 100) inserted into the ventrolateral quadrants of cervical segments 3 to 7. In twelve experiments, cathodal microstimulation (10–100 $\mu$A) of the dorsal respiratory group was also performed, proper placement of the microelectrode being ascertained by both stereotaxic co-ordinates and recordings of respiratory activity through the same electrode. In seven experiments, the main cervical branch of the glossopharyngeal nerve and/or the pharyngeal branch of the vagus nerve were also stimulated (0·5–4·0 V) in order to identify motoneurones of the pharyngeal muscles.

For each neurone, the membrane potential was defined as the difference between intracellular and extracellular potentials, using as a reference a single grounded silver–silver chloride electrode inserted into the scalp muscles. All measurements were corrected, if necessary, by measuring the extracellular potential in the vicinity of the neurone after the microelectrode was withdrawn from the cell.

*Histological procedure and morphological examination*

For intracellular staining, HRP was electrophoretically ejected from the microelectrode into the neurone using constant current of 2–10 nA, electrode tip positive, for 5–10 min. Membrane and action potentials were monitored during injection. After survival periods of 1–3 h to allow diffusion

of the enzyme, the abdominal aorta was clamped and the cats perfused via a cannula inserted into the left ventricle with buffered saline and a fixative solution. After post-fixation for 12 h and immersion in phosphate buffer with 30% sucrose for 24 h, frozen serial sections (50 $\mu$m) were made in the frontal plane. The HRP reaction product was visualized with a mixture of pyrocatechol and *p*-phenilenediamine (Hanker–Yates reagent, Sigma) following the method described by Hanker, Yates, Metz & Rustioni (1977). Labelled neurones were reconstructed using a microscope equipped with a camera lucida.

## RESULTS

Data were obtained from sixty-three respiratory neurones in which the resting membrane potentials were stable for 5 min to 1 h. Membrane potentials, during the phase of maximum hyperpolarization, averaged $58{\cdot}7 \pm 16{\cdot}5$ (S.D.) mV (range $-40$ to $-80$ mV) with KCl-filled microelectrodes (thirty-nine neurones), and $47{\cdot}3 \pm 12{\cdot}6$ mV (range $-30$ to $-60$ mV) with HRP-filled microelectrodes (twenty-four neurones). Five of the latter had membrane potentials of $-30$ mV, the minimum acceptable value. These were considered acceptable for inclusion in our study because (*a*) their patterns of change in membrane potential were similar to those of other neurones, (*b*) their membrane potentials were stable, and (*c*) ionophoresis of HRP produced adequate labelling.

### *Discharge patterns and membrane potentials of expiratory neurones*

Thirty-eight expiratory neurones were identified by a consistent membrane depolarization during the intervals between phrenic bursts. Some neurones discharged rhythmically during expiration before impalement and for only a few minutes following impalement. Others displayed expiratory spiking throughout the duration of study. Based on both the trajectories of their membrane potentials during the respiratory cycle and their discharge patterns, we classified the expiratory neurones into two groups. Twenty-two neurones, referred to as augmenting expiratory neurones, exhibited a progressive membrane depolarization during the interval between phrenic bursts, peak depolarization and discharge frequency occurring just before the onset of inspiration. In four of these, only a slight progressive depolarization and infrequent spike activity was evident during expiration. In contrast, sixteen neurones exhibited an abrupt and maximal depolarization soon after phrenic activity peaked; this was followed by a progressive repolarization of the membrane during the interval between phrenic bursts. These are termed post-inspiratory neurones (Richter, 1982; Remmers *et al.* 1985*b*).

*Augmenting expiratory neurones.* Figure 1 shows recordings of the membrane potentials of two augmenting expiratory neurones shortly after impalement with KCl-filled microelectrodes. A step depolarization occurred at the onset of expiration and was followed by a progressively increasing depolarization throughout expiration; this depolarization reached its peak shortly before the onset of phrenic discharge (Fig. 1*D*). In four neurones, only a weak depolarization occurred during the interval between phrenic bursts (Fig. 1*A*). Three of these neurones did not discharge, nor could they be antidromically activated.

All augmenting expiratory neurones rapidly hyperpolarized at the onset of inspiration. The membrane potential then either continued to fall, reaching a minimum value coincident with peak phrenic nerve activity (Fig. 1*D*) or remained

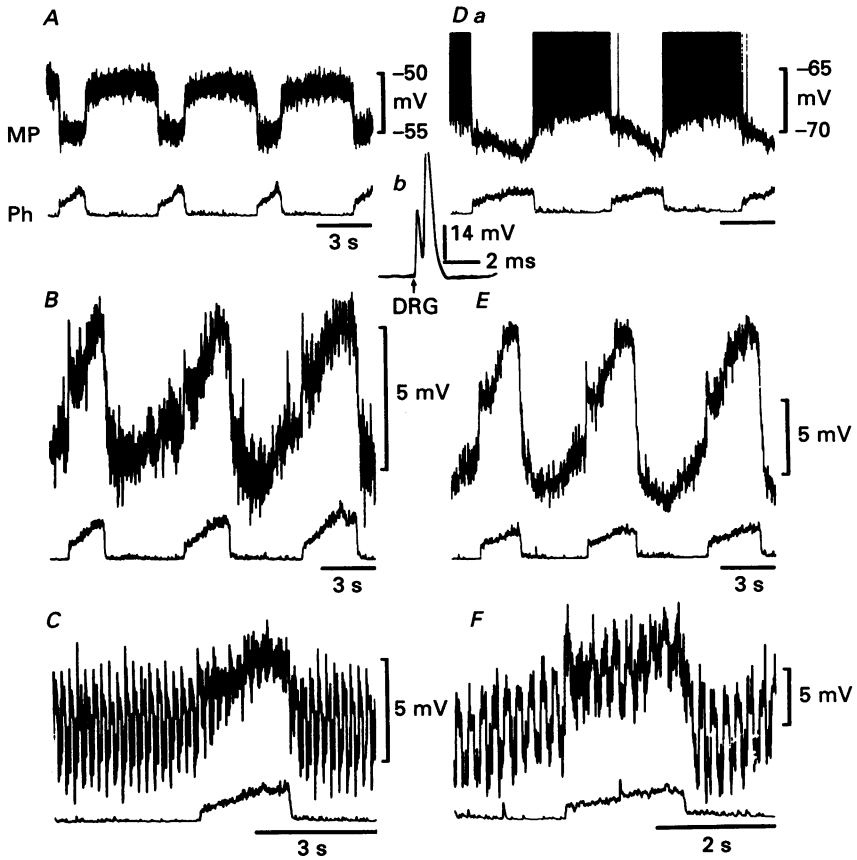


Fig. 1. Rhythmic changes of membrane potential (MP) of two augmenting expiratory neurones. In each panel membrane potentials obtained with KCl-filled microelectrodes are shown with integrated phrenic nerve activity (Ph). A–C, activity from a non-spiking neurone. *A*, control immediately after impalement. Note that over the three cycles depicted, a small depolarization appeared at end-inspiration due to a leak of chloride from the electrode. *B*, changes in membrane potential after chloride injection (−5 nA, 10 min; current off for recording). *C*, voltage responses of the neurone to −2 nA, 200 ms current pulses. *D–F*, activity of a spiking neurone. *Da*, just after impalement. *Db*, antidromic activation by contralateral stimulation of the DRG (arrow). *E*, changes in membrane potential after chloride injection (−5 nA, 12 min: current off for recording). *F*, voltage responses of the neurone to −2 nA, 200 ms current pulses.

at a steady value throughout inspiration. In the example of Figure 1*A*, the membrane depolarized slightly during inspiration. This may have been due to leakage of chloride into the cell following impalement and is consistent with the changes of membrane potential during the three respiratory cycles depicted. The temporal patterns of changes in membrane potential and spike activity were similar to those reported for expiratory bulbospinal neurones of the caudal medulla (Salmoiraghi & von Baumgarten, 1961; Mitchell & Herbert, 1974; Ballantyne & Richter, 1986).

Chloride was transferred from the micropipette into the cells by negative current

injections (−3 to −6 nA) for approximately 10 min; typical changes in the trajectories of membrane potentials are shown in Fig. 1*B* and *E*. This shift in equilibrium potential for chloride reversed the inspiratory hyperpolarizing waves during inspiration to depolarizing waves, indicating the presence of chloride-dependent inhibitory postsynaptic potentials (IPSPs) during inspiration. Such changes were observed in eight of the thirteen augmenting expiratory neurones from which recordings were made with KCl-filled microelectrodes. After reversal of

TABLE 1. Antidromic responses of different types of rostral medullary neurones to stimulation of various sites or nerves. Data expressed as number of positive responses (first number) per number of cells tested

| Neuronal type ($n = 63$) | Site of stimulation | | | | |
|---|---|---|---|---|---|
| | Spinal cord | DRG | SLN | Phar | Vagus |
| Expiratory neurones: | | | | | |
| Augmenting, $n = 13$ (KCl)+9 (HRP) | 3/17 | 2/17 | 0/17 | 1/8 | 0/17 |
| Post-inspiratory, $n = 9$ (KCl)+7 (HRP) | 0/15 | 0/4 | 0/16 | 0/5 | 0/16 |
| Inspiratory neurones: | | | | | |
| Augmenting, $n = 9$ (KCl)+6 (HRP) | 0/15 | 0/9 | 3/15 | 3/5 | 0/15 |
| Early burst, $n = 8$ (KCl)+2 (HRP) | 0/10 | 0/7 | 0/10 | 0/3 | 0/10 |

Abbreviations: HRP, HRP-filled microelectrodes; KCl, KCl-filled microelectrodes; DRG, dorsal respiratory group; SLN, ipsilateral superior laryngeal nerve; Phar, ipsilateral pharyngeal nerves (main cervical branch of glossopharyngeal nerve or pharyngeal branch of vagus nerve); Vagus, ipsilateral cervical vagus nerve.

inspiratory IPSPs was well developed, two separate waves of IPSPs were apparent: an early component followed by a later one which paralleled the increase in phrenic activity (Fig. 1*E*). In these augmenting expiratory neurones, we did not observe large post-inspiratory IPSPs reversed by chloride injection as previously described in expiratory neurones with similar discharge patterns but in the caudal medulla (Ballantyne & Richter, 1986). However, close examination of the membrane potential trajectory of one neurone (Fig. 1*B*) revealed less post-inspiratory repolarization, which may indicate a period of weak inhibition. The presence of effective postsynaptic inhibition was also manifested by a decrease during inspiration of the changes in membrane potential in response to constant-current pulses (Fig. 1*C* and *F*).

Of seventeen augmenting expiratory neurones tested for antidromic invasion, two were antidromically activated (latencies 0·6 and 2·3 ms) by electrical microstimulation of the contralateral dorsal respiratory group (DRG) in the caudal medulla, and three (latencies 1·5, 1·9 and 3·1 ms) by stimulation of the contralateral cervical spinal cord (Table 1). Eight neurones of the same sample were also tested by stimulation of the pharyngeal nerves, but only one was activated antidromically (latency 1·1 ms). None was activated by stimulation of the ipsilateral cervical vagus nerve or superior laryngeal nerve.

Stimulation of the superior laryngeal nerve evoked short-latency (5·0–8·0 ms)

waves of excitatory postsynaptic potentials (EPSPs) in three of nine augmenting neurones tested. The amplitude of these waves varied during the respiratory cycle, being larger in inspiration when the membrane was hyperpolarized (Fig. 2*D*) and smaller in expiration when the membrane was depolarized (Fig. 2*C*). This modulation of the amplitude of the responses might have been due either to a summation of these

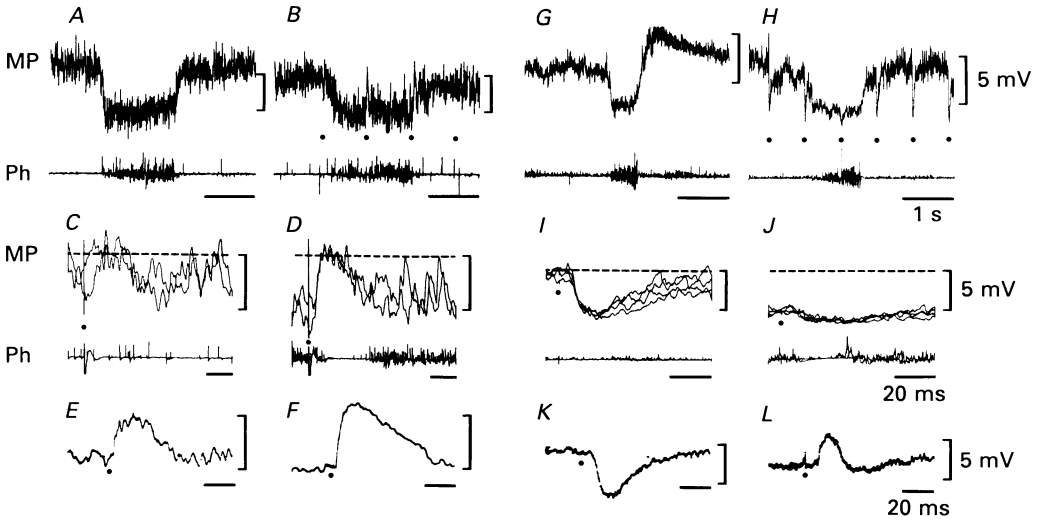


Fig. 2. Responses of expiratory neurones to superior laryngeal nerve (SLN) stimulation. Upper traces, membrane potential (MP); lower traces, phrenic nerve activity (Ph). *A–F*, activity of an augmenting expiratory neurone (same neurone as in Fig. 1*A*). *A*, control; *B*, stimulation of SLN (dots; 3 V, 0·1 ms; twice threshold for phrenic response). *C* and *D*, short-latency excitatory responses in expiration (*C*) or in inspiration (*D*), two superimposed traces. *E*, averaged EPSPs ($n = 4$) to SLN stimulation in inspiration or expiration. *F*, averaged EPSPs ($n = 4$) to SLN stimulation after chloride injection (−5 nA, 10 min; current off for recordings). *G–L*, post-inspiratory neurone. *G*, control. *H*, stimulation of SLN (dots; 2·5 V, 0·1 ms; twice threshold for phrenic response). *I* and *J*, short-latency inhibitory responses in expiration (*I*) or in inspiration (*J*). Four superimposed traces. Dashed horizontal lines in traces *C*, *D*, *I* and *J* indicate mean membrane potential in expiration. *K*, averaged IPSPs ($n = 4$) to SLN stimulation in expiration. *L*, averaged reversed IPSPs ($n = 4$) to SLN stimulation in expiration after chloride injection (−6 nA, 12 min; current off for recordings). Time scale in *A*, *B*, *G* and *H*, 1 s; in all other traces, 20 ms. Ordinate scale, 5 mV.

inputs with the disinhibition occurring in inspiration or to a presynaptic mechanism. In addition, we observed that these EPSPs were followed by a small hyperpolarization apparent during expiration (Fig. 2*C*). The prolongation of EPSPs in Fig. 2*F* compared to that in Fig. 2*E* might have been due to reversal of a hyperpolarization by chloride injection.

*Post-inspiratory neurones.* Figure 3 shows the membrane potentials of two post-inspiratory neurones obtained shortly after impalement with KCl-filled microelectrodes. These neurones displayed decrementing patterns of discharge, but others ceased firing a few minutes after impalement. In all post-inspiratory neurones, depolarization occurred abruptly immediately following the end of inspiration; thereafter, they either repolarized slowly ($n = 6$) throughout expiration (Fig. 3*A*) or

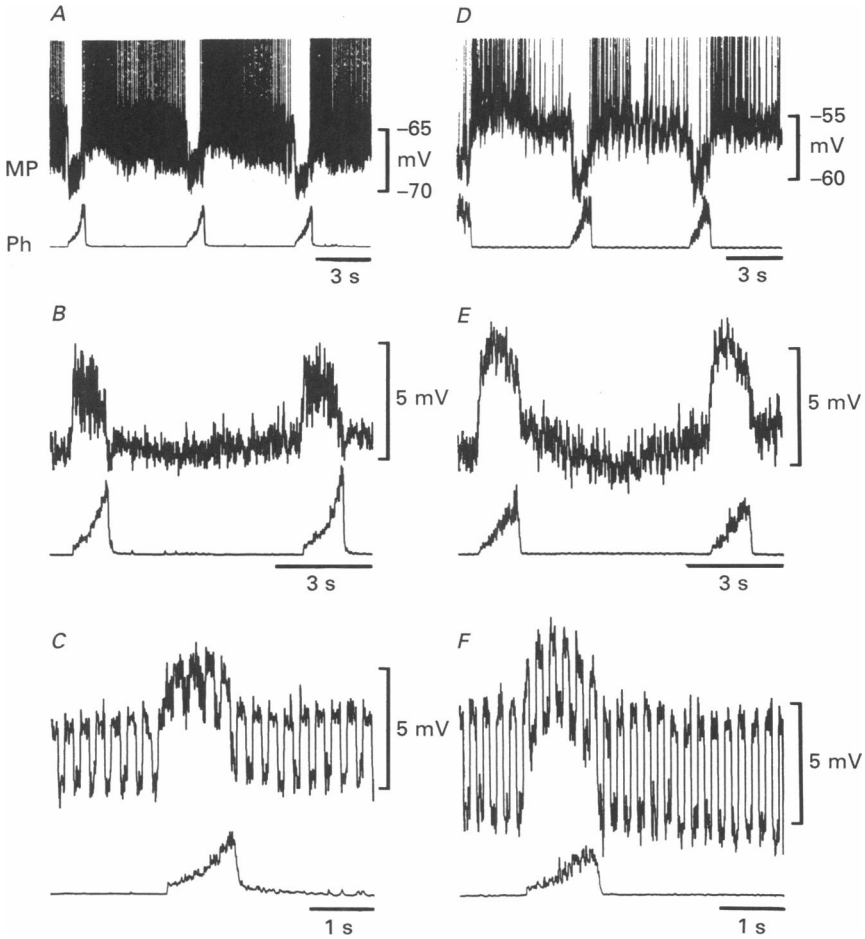


Fig. 3. Changes in membrane potentials (MP) of two post-inspiratory neurones. In each panel, membrane potentials obtained with KCl-filled microelectrodes are shown together with integrated phrenic nerve activity (Ph). *A–C*, activity from a spiking neurone with a decrementing discharge pattern throughout expiration. *A*, control just after impalement. *B*, membrane potential after chloride injection (−4 to −6 nA, 20 min; current off for recording). *C*, voltage responses of the neurone to −2 nA, 200 ms current pulses. *D–F*, activity from a neurone with lower discharge frequency. *D*, control. *E*, membrane potential after chloride injection (−4 nA, 10 min; current off for recordings). *F*, voltage responses to −2 nA, 200 ms current pulses.

remained at this level ($n = 10$) even though spike activity, when present, decreased in frequency (Fig. 3*D*). All neurones hyperpolarized rapidly at the onset of inspiration, the membrane potential depolarizing slightly during inspiration (Fig. 3*A* and *D*). These changes in membrane potential are similar to those of both post-inspiratory neurones of the caudal medulla (Richter, 1982; Remmers, Richter, Ballantyne, Bainton & Klein, 1985*a*, 1986), and of early expiratory laryngeal motoneurones (Richter, Heyde & Gabriel, 1975; Barillot, Bianchi & Gogan, 1984).

Intracellular chloride ionophoresis by steady currents (−3 to −7 nA) for

approximately 15–30 min progressively reversed the waves of hyperpolarization during the inspiratory phase (Fig. 3*B*). Ultimately, this evolved into a large depolarizing wave during inspiration, presumably the result of displacing the equilibrium potential for chloride to a more positive value (Fig. 3*B* and *E*). This reversal in the membrane potential was restricted to the period of phrenic activity. Brief hyperpolarizing constant-current pulses caused smaller changes in membrane potential during inspiration, indicating a lower input resistance during this phase (Fig. 3*C* and *F*). These changes in membrane potential, before and after chloride injection, were observed in six of the nine post-inspiratory neurones from which recordings were made with KCl-filled microelectrodes.

None of the sixteen post-inspiratory neurones tested was antidromically activated by stimulation of the cervical spinal cord, cervical vagus nerve, or superior laryngeal nerve. In addition, none of the five neurones of the same sample tested by stimulation of the pharyngeal nerves was antidromically activated (Table 1). In contrast to the synaptic excitation observed in some augmenting expiratory neurones, stimulation of the superior laryngeal nerve elicited in five of twelve post-inspiratory neurones short-latency (range 5·5–12·7 ms) IPSPs (Fig. 2*G–L*). Stimulation of pharyngeal nerves elicited IPSPs in two neurones (latencies 6·0–15·0 ms). In only one neurone did stimulation of both the superior laryngeal and pharyngeal nerves elicit an IPSP. The amplitudes of the IPSPs varied during the respiratory cycle (Fig. 2*H*), being smaller in inspiration (Fig. 2*J*) when the membrane was hyperpolarized and larger in expiration (Fig. 2*I*) when the membrane was depolarized. Chloride injection reversed the polarity of these IPSPs (Fig. 2*K* and *L*).

*Discharge patterns and membrane potentials of inspiratory neurones*

Twenty-five inspiratory neurones were identified by depolarization of their membranes during the phrenic burst. Two types of inspiratory neurones were observed. Fifteen exhibited progressive depolarization of the membrane, resulting in an augmenting discharge pattern similar to that reported for augmenting inspiratory neurones of the dorsal and ventral respiratory groups in the caudal medulla (Bianchi, 1974; Richter *et al.* 1975; Ballantyne & Richter, 1984). The other ten displayed an abrupt depolarization at the onset of the phrenic burst followed by a progressive repolarization and a decreasing discharge frequency during inspiration. They were classified as decrementing inspiratory neurones and their behaviour resembles that of early burst inspiratory neurones located in the ventral respiratory group of the caudal medulla (Bianchi, 1974; Merrill, 1974).

*Augmenting inspiratory neurones.* These neurones displayed a step membrane depolarization at the onset of phrenic activity and a progressive membrane depolarization throughout inspiration, reaching a maximum coincident with (Fig. 4*A* and *E*) or just before (Fig. 5) peak phrenic activity. At end-inspiration, the cell membrane rapidly repolarized before peak phrenic activity (Fig. 5) or during the period between the peak and the end of phrenic nerve activity (Fig. 4*A* and *E*), a period referred to as the first stage of expiration (Richter, 1982; Remmers *et al.* 1986). Thereafter, the membrane either depolarized progressively throughout expiration (Fig. 4*E*), or depolarized in mid-expiration, repolarizing just before the

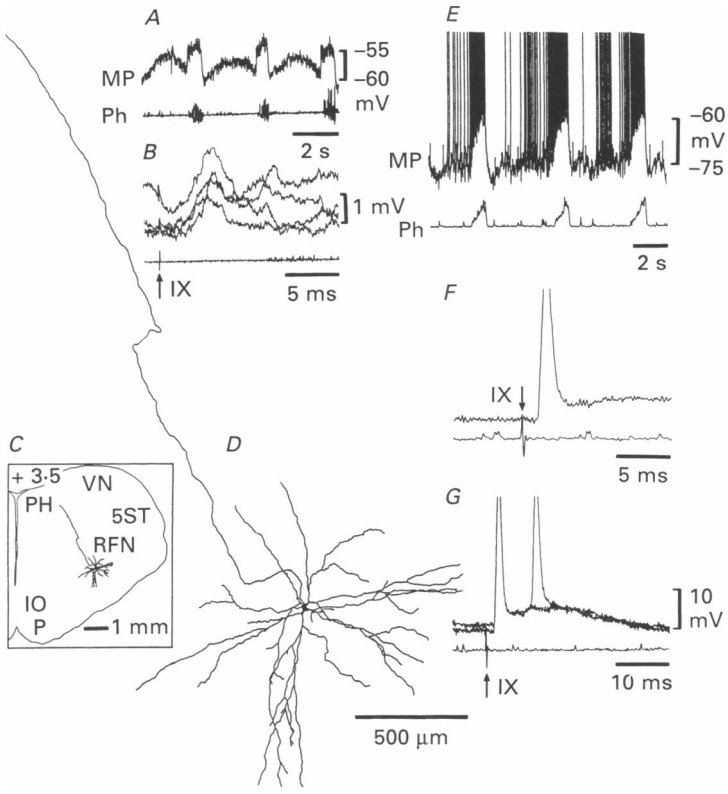


Fig. 4. Membrane potentials (MP) and morphology of inspiratory neurones of the retrofacial nucleus. Membrane potentials were recorded with HRP-filled microelectrodes. In panels *A*, *B*, *E*, *F* and *G* upper traces are membrane potentials; lower traces, raw phrenic nerve activity (Ph) except in panel *E* where it is integrated phrenic nerve activity. *A*, control activity of a non-spiking neurone. *B*, four superimposed traces of short-latency EPSPs obtained for the same neurone shown in *A* during stimulation of the glossopharyngeal nerve (arrow, IX). *C*, location of this neurone in the retrofacial nucleus as indicated in *D* (transverse section of medulla 3·5 mm rostral to the obex). *E*, control activity of a spiking neurone inadequately stained for reconstruction but located within the retrofacial nucleus 5·5 mm rostral to the obex. *F*, antidromic activation of this neurone by stimulation of the glossopharyngeal nerve (arrow, IX). *G*, two superimposed traces at slower time base during stimulation of the glossopharyngeal nerve (arrow, IX) showing both antidromic response and synaptic excitation. Abbreviations: 5ST, spinal trigeminal tract; IO, inferior olive; P, pyramidal tract; PH, nucleus praepositus hypoglossi; RFN, retrofacial nucleus; VN, vestibular nucleus.

onset of inspiration (Fig. 4*A*). This latter pattern has been observed in inspiratory laryngeal motoneurones (J. C. Barillot, L. Grélot, S. Reddad & A. L. Bianchi, unpublished observations). In nine augmenting inspiratory neurones from which recordings were made with KCl-filled microelectrodes, intracellular ionophoresis of chloride did not reverse unambiguously the late expiratory hyperpolarization. However, in two neurones antidromically activated by stimulation of the superior laryngeal nerve, ionophoresis of chloride reversed the wave of IPSPs observed during the first stage of expiration (Fig. 5*D* and *E*).

Fifteen augmenting inspiratory neurones were tested for antidromic invasion by stimulation of the spinal cord and the ipsilateral cervical vagus nerve, and nine were tested for antidromic invasion by microstimulation of the contralateral DRG. None was antidromically activated (Table 1). Of this sample of fifteen neurones, three were antidromically activated by stimulation of the superior laryngeal nerve (latencies 1·3–1·9 ms), and three of five tested by stimulation of the pharyngeal nerves (latencies 1·2–1·5 ms) (Figs 4*F*, 4*G* and 7*C*).

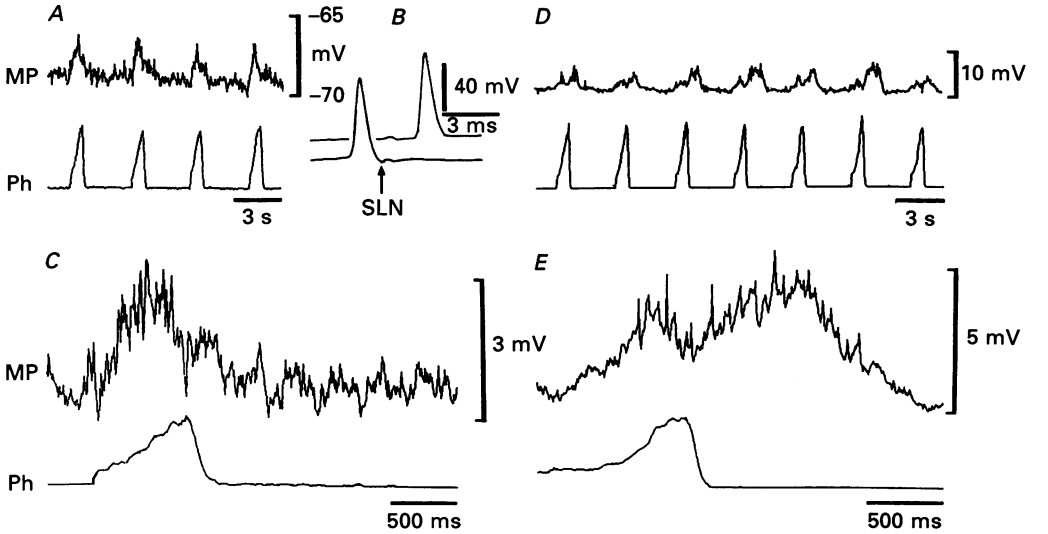


Fig. 5. Changes in membrane potential (MP) of an inspiratory neurone antidromically activated by superior laryngeal nerve stimulation. Upper traces are membrane potentials (MP) obtained with a KCl-filled microelectrode (spikes suppressed during A/D conversion). Lower traces are integrated phrenic nerve activity (Ph). *A*, control. *B*, antidromic activation following SLN stimulation (arrow, SLN); lower trace shows failure of antidromic potential when spontaneous spike preceded stimulation. *C*, computer-averaged membrane potential and integrated phrenic nerve activity of seven respiratory cycles, four of which are shown in *A*. *D*, changes in membrane potential after chloride injection (−5 nA, 10 min; current off for recording). *E*, computer-averaged membrane potential and integrated phrenic nerve activity of the seven respiratory cycles shown in *D*.

Stimulation of pharyngeal nerves also induced short-latency (7·0–8·0 ms) EPSPs in three of nine neurones tested (Fig. 4*B*, 4*G* and 7*C*). In addition, in the two neurones with pharyngeal axons, stimulation of the superior laryngeal nerve also evoked EPSPs (latencies 4·9 and 5·4 ms) followed by a hyperpolarization (latency 13·6 ms) in one of them (Fig. 7*E*). No synaptic responses were observed for the three motoneurones with axons in the superior laryngeal nerve.

*Early burst inspiratory neurones.* Stable intracellular recordings were obtained with KCl-filled microelectrodes in eight neurones of this type, and in two with HRP-filled microelectrodes. All were tested for antidromic invasion following stimulation of the spinal cord and superior laryngeal nerve, seven by microstimulation of the contralateral DRG, and three by stimulation of the pharyngeal nerves (Table 1).

None could be antidromically activated. However, in one of three neurones tested by stimulation of the superior laryngeal nerve, a short-latency (10 ms) depolarization resulted.

The membranes of these neurones depolarized abruptly at the onset of inspiration, and then repolarized slowly throughout inspiration (Fig. 6*A*). Some neurones displayed a decrementing discharge pattern during inspiration. Membrane repolarization was rapid and coincided with peak phrenic activity, membrane potentials

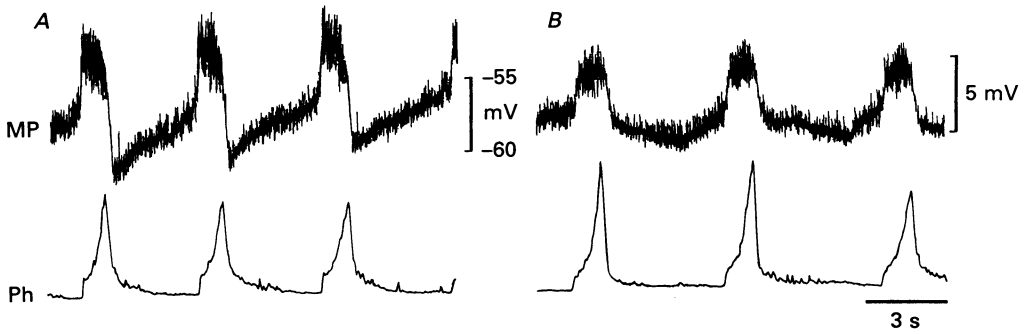


Fig. 6. Changes in membrane potential (MP) of an early burst inspiratory neurone. Ph, integrated phrenic nerve activity. Membrane potential recorded with a KCl-filled microelectrode. *A*, control. *B*, reversal of the transient hyperpolarization in post-inspiration after chloride injection (−4 nA, 5 min; current off for recording).

reaching minimum values in early expiration. Thereafter, they depolarized during expiration. Inspiratory interneurones with similar patterns of changes in membrane potential have been previously described in the caudal medulla (Merrill, 1974; Richter, 1982). After intracellular ionophoresis of chloride (−10 nA for 10 min), there was still an abrupt repolarization at the onset of expiration (Fig. 6*B*). The trajectory of the change in membrane potential during the interval between phrenic bursts revealed two components: a declining trajectory during the first stage of expiration (the post-inspiratory phase) followed by a depolarization during the rest of expiration. In other words, the abrupt hyperpolarization at the beginning of the first stage was reduced by chloride injection, indicating that the hyperpolarization was partially due to a barrage of IPSPs. Comparison of Fig. 6*A* and *B* also reveals a reduction of repolarization in late inspiration after chloride injection. This suggests that inspiratory IPSPs contributed to the slight hyperpolarization trajectory during inspiration in early burst inspiratory neurones.

*Location and morphology of inspiratory neurones*

We impaled six augmenting inspiratory neurones and two early burst inspiratory neurones with HRP-filled microelectrodes. The somata of four augmenting neurones and one early inspiratory neurone were successfully stained and reconstructed. Three augmenting inspiratory neurones lay in the retrofacial nucleus; two were antidromically activated by stimulation of the glossopharyngeal nerve (Figs 4*E* and 7). One was not antidromically activated by stimulation of the glossopharyngeal nerve (Fig. 4*A–D*). However, it was probably a pharyngeal motoneurone due to both its

somal location and the path of its axon (Fig. 4*C* and *D*). Two reconstructed neurones had stellate somata, 30–40 $\mu$m in diameter, giving off seven to eight dendritic trunks, each ramifying into branches extending up to 700 $\mu$m in every direction. Their axons first ran dorsomedially, could be followed for 2 mm, and had no axon collaterals. Reconstruction of another augmenting neurone (Fig. 8*A*) revealed a stellate soma,

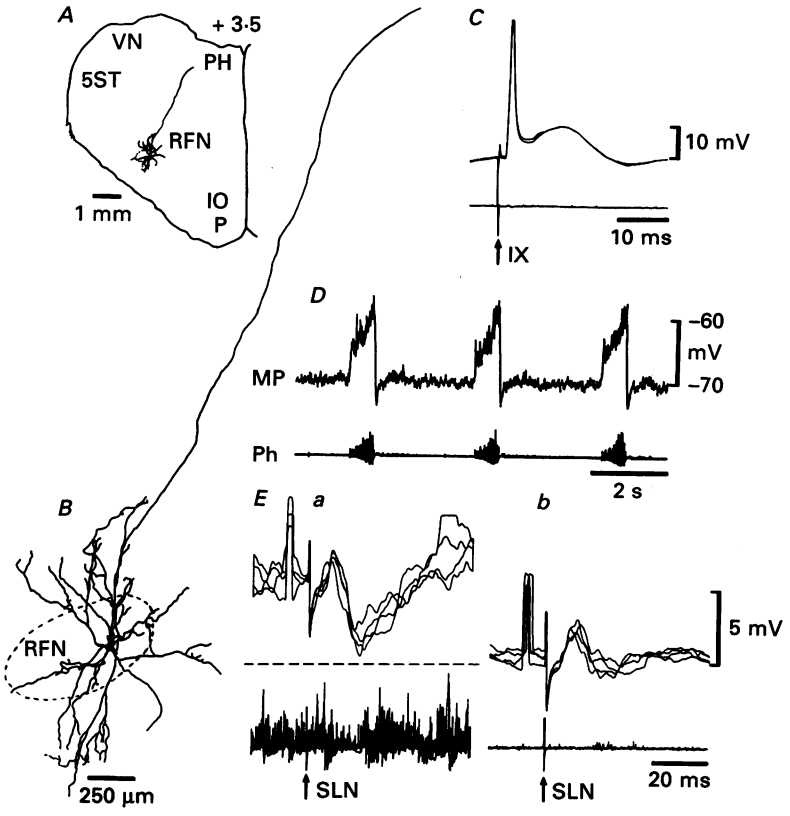


Fig. 7. Membrane potential (MP) and morphology of an inspiratory neurone of the retrofacial nucleus. HRP-filled microelectrode. *A*, transverse section of the medulla 3·5 mm in front of the obex. *B*, reconstruction of neurone, location of which is given in *A*. Panels *C*, *D* and *Ea* and *b* upper traces are membrane potentials (MP); lower traces are raw phrenic nerve activity (Ph). *C*, antidromic activation followed by an EPSP after glossopharyngeal nerve stimulation (arrow, IX). *D*, control activity. *Ea* and *b*, four superimposed traces during stimulation of the superior laryngeal nerve (arrow, SLN) in early inspiration (*a*) and late expiration (*b*). Dotted line in *a* is the average membrane potential in expiration. Calibration pulses, 5 mV, 2 ms. Abbreviations as in Fig. 4.

40 × 50 $\mu$m in diameter, in the facial nucleus and giving off seven dendritic trunks with profuse branchings into fine ramifications. Most of the dendritic branches remained within the facial nucleus and could be followed for over 700 $\mu$m in every direction, but with a prominent dorsolateral and ventromedial orientation. The axon of this neurone was not identified.

The early inspiratory neurone was also located dorsal to the caudal portion of the facial nucleus. It had a fusiform soma (60 × 20 $\mu$m), giving off four large dendritic

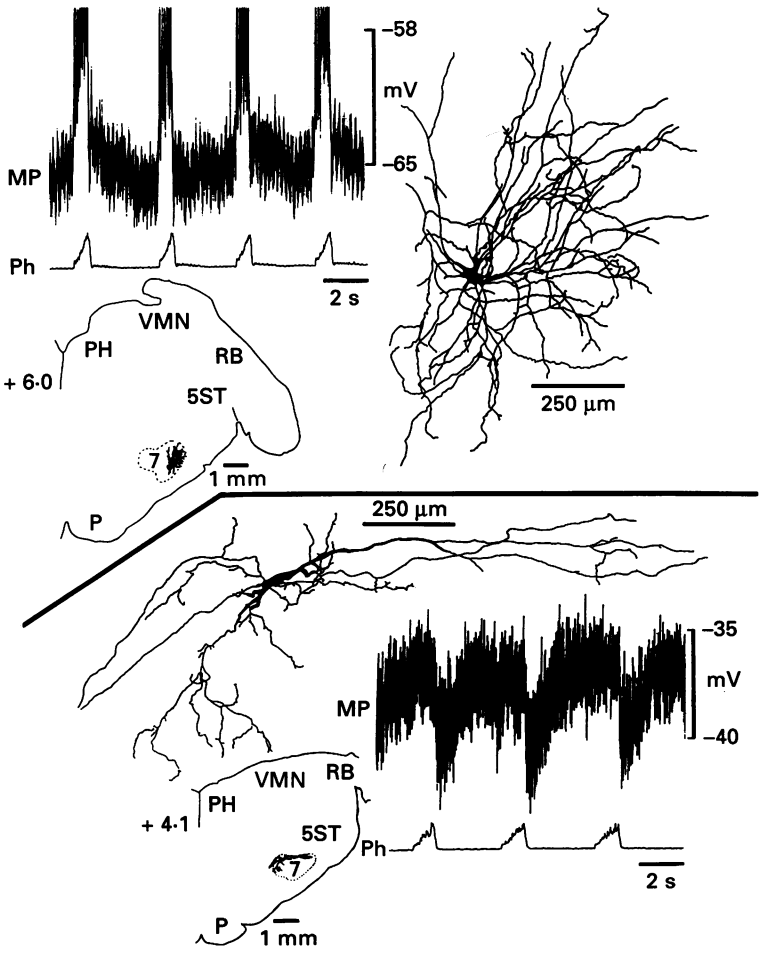


Fig. 8. Membrane potentials (MP) and morphology of two inspiratory neurones, the somata of which were located in the caudal facial nucleus. HRP-filled microelectrodes. *A*, augmenting neurone, soma 6·0 mm rostral to the obex. *B*, early burst inspiratory neurone soma in the dorsal region of caudal facial nucleus, 4·1 mm rostral to the obex. Note caudal position of the facial nucleus in this small (2·2 kg) cat. Abbreviations: 7, motor nucleus of the facial nerve; RB, restiform body; other abbreviations as in Fig. 4.

trunks which branched into fine ramifications in the ventromedial and lateral directions. Some of these branches extended more than 1000 μm (Fig. 8*B*). No axon was found outside the limit of the nucleus.

## DISCUSSION

This report provides the first intracellular analysis of membrane potential trajectories and postsynaptic activities of respiratory neurones of the rostral medulla in the region of the retrofacial nucleus. We also describe excitatory and inhibitory synaptic inputs that influence their activities and we correlate these functional properties with morphological characteristics.

We explored a region of the rostral medulla that includes the so-called 'Bötzinger Complex', consisting mainly of augmenting expiratory neurones discharging at high frequencies in late expiration (Lipski & Merrill, 1980; Fedorko & Merrill, 1984). Our findings confirm previous results (Bianchi & Barillot, 1982; Remmers *et al.* 1985*b*; Bianchi, Barillot & Grélot, 1986), demonstrating a variety of respiratory neurones in the region of the retrofacial nucleus in decerebrate cats. These neuronal types include decrementing inspiratory neurones, post-inspiratory neurones, and augmenting inspiratory neurones. Most appeared to be propriobulbar interneurones but pharyngeal motoneurones constitute a subpopulation of three neuronal types: augmenting expiratory, post-inspiratory and augmenting inspiratory neurones.

Our results, therefore, indicate the presence of several functional types of expiratory neurones in the rostral medulla. One type corresponded to motoneurones of the retrofacial nucleus with either an augmenting or post-inspiratory pattern of activity (discharge or membrane potential) and not exclusively a 'plateau' as reported by Otake, Sasaki, Mannen & Ezure (1987). Another consists of expiratory interneurones with augmenting discharge patterns and located either ventromedial to the retrofacial nucleus or near the ventral surface of the medulla, (Grélot, Bianchi, Iscoe & Remmers, 1988).

The observed rhythmic changes in the membrane potentials of augmenting expiratory neurones consisting of hyperpolarizations due to chloride-dependent IPSPs during inspiration alternating with augmenting depolarizations during expiration, resembled those of expiratory bulbospinal neurones in the caudal medulla (Mitchell & Herbert, 1974; Richter, 1982; Ballantyne & Richter, 1986; Arita, Kogo & Koshiya, 1987). Both early and late waves of postsynaptic inhibition were observed during inspiration (Fig. 1), the former being smaller than the latter. The early inhibition may have originated from early burst inspiratory neurones lying in the ventral respiratory group (Merrill, 1974; Bianchi, 1974; Richter, 1982; Ballantyne & Richter, 1986) or near the retrofacial nucleus (Bianchi & Barillot, 1982), and the late inhibition from augmenting inspiratory neurones of the dorsal respiratory group, ventral respiratory group or both.

Despite these similarities in the patterns of discharge of caudal and rostral augmenting expiratory neurones, some rostral neurones displayed synaptic responses to stimulation of the laryngeal afferents that differed from those typical of caudal expiratory neurones. Some of the former were excited at short latency (Fig. 2*A–F*), whereas caudal expiratory neurones are inhibited, by stimulation of afferents in the superior laryngeal nerve (Ballantyne & Richter, 1986). When stimulation occurred during inspiration, part of the depolarization probably reflected disinhibition secondary to the inhibition of inspiratory neurones which themselves inhibit these expiratory neurones. These opposing responses of rostral and caudal augmenting expiratory neurones to superior laryngeal nerve stimulation are reminiscent of the differences between post-inspiratory neurones in the rostral and caudal medulla. Post-inspiratory neurones in the ventral respiratory group of the caudal medulla are excited at short latency by stimulation of superior laryngeal nerve afferents (Remmers *et al.* 1985*a*), whereas post-inspiratory neurones of the retrofacial region were inhibited (Fig. 2*G–L*).

Some inspiratory neurones of our study were probably motoneurones innervating the posterior cricothyroid muscle, since they were antidromically activated by

stimulation of the superior laryngeal nerve. Their stereotaxic co-ordinates suggested that they lay in the rostral pole of the nucleus ambiguus (Lawn, 1966). Several lines of evidence indicate that some others were probably pharyngeal motoneurones. First, they could be antidromically activated by stimulation of the glossopharyngeal nerve or pharyngeal branch of the vagus nerve. Second, reconstructions revealed several somata in the retrofacial nucleus itself, with axons following the roots of the cranial nerves (Grélot *et al.* 1988). Third, the discharge patterns of some rostral expiratory and inspiratory neurones in our study were similar to those of single fibres in the glossopharyngeal and pharyngeal nerves (Barillot, Bianchi, Grélot, Pio & Roman, 1987). The responses of these pharyngeal motoneurones to stimulation of laryngeal afferents are opposite to those of laryngeal motoneurones; IPSPs were elicited in post-inspiratory motoneurones and EPSPs in inspiratory pharyngeal motoneurones, while expiratory and inspiratory laryngeal motoneurones display EPSPs and IPSPs, respectively, to activation of the same afferents (see e.g. Barillot *et al.* 1984). These responses may be important in the control of upper-airway calibre both in normal breathing and in circumstances in which laryngeal receptors are activated.

The existence of pharyngeal motoneurones and interneurones in the facial nucleus may explain the anaesthesia-induced reduction of respiratory-related activity of some neurones in the rostral region of the medulla (Grélot & Bianchi, 1987). Hwang, St John & Bartlett (1983) have shown that anaesthesia suppresses upper-airway respiratory motor activities much more than those of the bulbospinal respiratory complex.

Some expiratory neurones in our study were ventromedial to the retrofacial nucleus or near the ventral surface of the medulla, and their dendrites terminated near the ventral surface of the medulla (Grélot *et al.* 1988). This region of the ventral medulla corresponds to the intermediate and caudal parts of the rostral chemosensitive areas (Mitchell, Loeschcke, Massion & Severinghaus, 1963; Loeschcke, De Lattre, Schlaefke & Trouth, 1970). This region may also coincide with the nucleus paragigantocellularis lateralis which, when cooled, causes apnoea or profound depression of inspiratory motor output (Budzinska, von Euler, Kao, Pantaleo & Yamamoto, 1985). It also overlaps that of the subretrofacial nucleus where bulbospinal neurones involved in the control of sympathetic preganglionic neurones are found (McAllen, 1986). Subretrofacial neurones exhibiting a respiratory modulation, mainly inspiratory, are part of the descending vasomotor pathway (McAllen, 1987). However, this same region of the ventral medulla receives afferent inputs from the nucleus of the tractus solitarius (Loewy & Burton, 1978; Andrezik, Chan-Palay & Palay, 1981) and may, therefore, be a site of convergence of peripheral and central chemoreceptor inputs. Additional experiments involving these rostral respiratory neurones with dendritic arbors near the ventral surface of the medulla should examine their role(s) in central chemoreception.

We are grateful to Stanley Schultz for excellent technical assistance in Calgary, and in Marseille, to Mrs J. Pio for histological preparation, Mrs J. Roman for preparation of the illustrations and Mrs M. Sellem and M. Schultz for typing the manuscript. This work was supported by the CNRS (UA 205), the Alberta Heritage foundation for Medical Research and the Medical Research Council of Canada.

REFERENCES

ANDREZIK, J. A., CHAN-PALAY, V. & PALAY, J. L. (1981). The nucleus paragigantocellularis lateralis in the rat. Demonstration of afferents by the retrograde transport of horseradish peroxidase. *Anatomy and Embryology* **161**, 373–390.

ARITA, H., KOGO, N. & KOSHIYA, N. (1987). Morphological and physiological properties of caudal medullary expiratory neurons of the cat. *Brain Research* **401**, 258–266.

BALLANTYNE, D. & RICHTER, D. W. (1984). Postsynaptic inhibition of bulbar inspiratory neurones in the cat. *Journal of Physiology* **348**, 67–87.

BALLANTYNE, D. & RICHTER, D. W. (1986). The non-uniform character of expiratory synaptic activity in expiratory bulbospinal neurones of the cat. *Journal of Physiology* **370**, 433–456.

BARILLOT, J. C., BIANCHI, A. L. & GOGAN, P. (1984). Laryngeal respiratory motoneurones: morphology and electrophysiological evidence of separate sites for excitatory and inhibitory synaptic inputs. *Neuroscience Letters* **47**, 107–112.

BARILLOT, J. C., BIANCHI, A. L., GRÉLOT, L., PIO, J. & ROMAN, J. (1987). Etude anatomique, morphologique et électrophysiologique des montoneurones des muscles du pharynx chez le chat. *Archives internationales de physiologie et de biochimie* (in the Press).

BATSEL, H. L. (1964). Localization of bulbar respiratory center by microelectrode sounding. *Experimental Neurology* **9**, 410–426.

BIANCHI, A. L. (1971). Localisation et étude des neurones respiratoires bulbaires. Mise en jeu antidromique par stimulation spinale ou vagale. *Journal de physiologie* **63**, 5–40.

BIANCHI, A. L. (1974). Modalités de décharge et propriétés anatomo-fonctionnelles des neurones respiratoires bulbaires. *Journal of physiologie* **68**, 555–587.

BIANCHI, A. L. (1985). Interconnective pathways between respiratory groups of neurons: results from electrophysiological experiments as opposed to anatomical tracing methods. In *Neurogenesis of Central Respiratory Rhythm*, ed. BIANCHI, A. L. & DENAVIT-SAUBIE, M., pp. 108–116. Lancaster: MTP Press.

BIANCHI, A. L. & BARILLOT, J. C. (1982). Respiratory neurons in the region of the retrofacial nucleus: pontile, medullary, spinal and vagal projections. *Neuroscience Letters* **31**, 277–282.

BIANCHI, A. L., BARILLOT, J. C. & GRÉLOT, L. (1986). Pattern of excitability of respiratory neurons in the region of the retrofacial nucleus. In *Neurobiology of the Control of Breathing*, ed. VON EULER, C. & LAGERCRANTZ, H., pp. 149–155. New York: Raven Press.

BIANCHI, A. L., GRÉLOT, L. & REMMERS, E. (1987). Morphological and electrophysiological identification of respiratory neurones in the region of the retrofacial nucleus. *Neuroscience* **22**, S394.

BUDZINSKA, K., VON EULER, C., KAO, F. F., PANTALEO, T. & YAMAMOTO, Y. (1985). Effects of graded focal cold block in rostral areas of the medulla. *Acta physiologica scandinavica* **124**, 329–340.

BYSTRZYCKA, E. K. (1980). Afferent projections to the dorsal and ventral respiratory nuclei in the medulla oblongata of the cats studied by the horseradish peroxidase technique. *Brain Research* **185**, 59–66.

FEDORKO, L. & MERRILL, E. G. (1984). Axonal projections from the rostral expiratory neurones of the Bötzinger complex to medulla and spinal cord in the cat. *Journal of Physiology* **350**, 487–496.

GRÉLOT, L. & BIANCHI, A. L. (1987). Differential effects of halothane anesthesia on the pattern of discharge of inspiratory and expiratory neurons in the region of the retrofacial nucleus. *Brain Research* **407**, 335–338.

GRÉLOT, L., BIANCHI, A. L., ISCOE, S. & REMMERS, J. E. (1988). Expiratory neurones of the rostral medulla: anatomical and functional correlates. *Neuroscience Letters* **89**, 140–145.

HANKER, J. S., YATES, P. E., METZ, C. B. & RUSTIONI, A. (1977). A new specific, sensitive and non carcinogenic reagent for the demonstration of horseradish peroxidase. *Histochemical Journal* **9**, 789–792.

HWANG, J. C., ST JOHN, W. M. & BARTLETT, J. D. (1983). Respiratory-related hypoglossal nerve activity: influence of anesthetics. *Journal of Applied Physiology* **55**, 785–792.

KALIA, M., FELDMAN, J. L. & COHEN, M. I. (1979). Afferent projections to the inspiratory neuronal region of the ventrolateral nucleus of the tractus solitarius in the cat. *Brain Research* **171**, 135–141.

KIRSTEN, E. B. & ST JOHN, W. M. (1978). A feline decerebration technique with low mortality and long term homeostasis. *Journal of Pharmacological Methods* **1**, 263–268.

LAWN, A. M. (1966). The nucleus ambiguus of the rabbit. *Journal of Comparative Neurology* **127**, 307–320.

LIPSKI, J. & MERRILL, E. G. (1980). Electrophysiological demonstration of the projection from expiratory neurones in rostral medulla to contralateral dorsal respiratory group. *Brain Research* **197**, 521–524.

LOESCHCKE, H. H., DE LATTRE, J., SCHLAEFKE, M. E. & TROUTH, C. O. (1970). Effects on respiration and circulation of electrically stimulating ventral surface of the medulla oblongata. *Respiration Physiology* **10**, 184–197.

LOEWY, A. D. & BURTON, H. (1978). Nuclei of the solitary tract: efferent projections to the lower brain stem and spinal cord of the cat. *Journal of Comparative Neurology* **181**, 421–449.

LONG, S. & DUFFIN, J. (1986). The neuronal determinants of respiratory rhythm. *Progress in Neurobiology* **27**, 107–182.

MCALLEN, R. M. (1986). Identification and properties of sub-retrofacial bulbospinal neurones: a descending cardiovascular pathway in the cat. *Journal of the Autonomic Nervous System* **17**, 151–164.

MCALLEN, R. M. (1987). Central respiratory modulation of subretrofacial bulbospinal neurones in the cat. *Journal of Physiology* **388**, 533–545.

MERRILL, E. G. (1970). The lateral respiratory neurones of the medulla: their associations with nucleus ambiguus nucleus retroambigalis, the spinal accessory nucleus and the spinal cord. *Brain Research* **24**, 11–28.

MERRILL, E. G. (1974). Finding a respiratory function of the medullary neurones. In *Essays on the Nervous System*, ed. BELLAIRS, R. & GRAYS, E. G., pp. 451–486. Oxford: Clarendon Press.

MERRILL, E. G., LIPSKI, J., KUBIN, L. & FEDORKO, L. (1983). Origin of the expiratory inhibition of nucleus tractus solitarius inspiratory neurones. *Brain Research* **263**, 43–50.

MITCHELL, R. A. & HERBERT, D. A. (1974). The effect of carbon dioxide on the membrane potential of medullary respiratory neurones. *Brain Research* **75** (2), 345–349.

MITCHELL, R. A., LOESCHCKE, H. H., MASSION, W. H. & SEVERINGHAUS, J. W. (1963). Respiratory responses mediated through superficial chemosensitive areas on the medulla. *Journal of Applied Physiology* **18**, 523–533.

OTAKE, K., SASAKI, H., MANNEN, H. & EZURE, K. (1987). Morphology of expiratory neurons of the Bötzinger complex: an HRP study in the cat. *Journal of Comparative Neurology* **258**, 565–579.

REMMERS, J. E., RICHTER, D. W., BALLANTYNE, D., BAINTON, C. R. & KLEIN, J. P. (1985*a*). Activation of bulbar post-inspiratory neurons by upper airway stimulation. In *Neurogenesis of Central Respiratory Rhythm*, ed. BIANCHI, A. L. & DENAVIT-SAUBIE, M., pp. 290–291. Lancaster: MTP Press.

REMMERS, J. E., RICHTER, D. W., BALLANTYNE, D., BAINTON, C. R. & KLEIN, J. P. (1986). Reflex prolongation of stage I of expiration. *Pflügers Archiv* **407**, 190–198.

REMMERS, J. E., TAKEDA, R., SCHULTZ, S. A. & HAJI, A. (1985*b*). Relationship of membrane potential of ventral respiratory group neurons to action potentials of retrofacial respiratory units. In *Neurogenesis of Central Respiratory Rhythm*, ed. BIANCHI, A. L. & DENAVIT-SAUBIE, M., pp. 117–120. Lancaster: MTP Press.

RICHTER, D. W. (1982). Generation and maintenance of the respiratory rhythm. *Journal of Experimental Biology* **100**, 93–107.

RICHTER, D. W., HEYDE, F. & GABRIEL, M. (1975). Intracellular recordings from different types of medullary respiratory neurons of the cat. *Journal of Neurophysiology* **38** (5), 1162–1171.

SALMOIRAGHI, G. C. & VON BAUMGARTEN, R. (1961). Intracellular potentials from respiratory neurons in the brain stem of the cat and mechanism of rhythmic respiration. *Journal of Neurophysiology* **24**, 203–218.

VON BAUMGARTEN, R., VON BAUMGARTEN, C. & SCHAEFFER, P. (1957). Beitrag zur Lokalisationsfrage bulboreticularer respiratorischer Neurone der Katze. *Pflügers Archiv* **264**, 217–227.

VON EULER, C., HAYWARD, J. N., MARTTILA, I. & WYMAN, R. J. (1973). Respiratory neurons of the ventrolateral nucleus of the solitary tract of cat: vagal input, spinal connections and morphological identification. *Brain Research* **61**, 1–22.